Rubber Elasticity of Cross-Linked Networks with Trapped Entanglements and Dangling Chains

Christos Tsenoglou

Department of Chemistry and Chemical Engineering, Stevens Institute of Technology, Hoboken, New Jersey 07030. *Received December 4, 1987; Revised Manuscript Received June 6, 1988*

ABSTRACT: This is a theoretical study on the effects of the network structure and deformation on the stress response of permanent elastomeric networks containing trapped entanglements and chain defects. In these systems, elastically active chains with both ends cross-linked coexist with segments that are tethered at one end only. It is assumed that under strain, internal strands preserve their deformation with time while dangling segments restore their initial length by retraction and continue their conformational renewal through chain fluctuations. The dynamics of the tethered branches cause disengagement of untrapped entanglements on neighboring segments, thus undermining the structural solidity of the elastomer. The calculated stress under constant deformation depends on the strain value, the molecular weight between cross-links and between entanglements, the relative participation of the tethered chains in the network, and the degree of the relaxation completion. The theory accommodates the observed deviations from neo-Hookean behavior, and the predicted effects of the network architecture are consistent with the experimental evidence.

Introduction

The mechanical properties of dense macromolecular systems are strongly affected by the large scale structure and stability of their polymeric network.[1] The material rigidity, for example, is proportional to the density of interchain associations, and the fluidity is a measure of the swiftness with which molecular configurations are renewed.

The present work attempts to explain the viscoelastic behavior of a general case of amorphous, unswollen rubber networks, where chains with both ends fixed coexist with tethered ones (Figure 1). The variety of molecular interactions generated by the coupling between internal and terminal segments complicates the study of these systems. Provided that the internal strands are sufficiently long, they couple with other strands and dangling chains. A trapped entanglement along an internal strand acts as a loose but indestructable cross-link. An entanglement caused by an interaction with a tethered chain, however, has a finite lifetime subject to the dynamics of the dangling end. The loss of these junctions during the relaxation of the terminal chains enchances the "fluid" character of the rubber and intensifies the dissipation of energy stored in the deformed network.

Structural Features of the Network

A permanent network can be formed from a polymer melt by random cross-linking. As the chemical change proceeds, temporary entanglements are replaced by permanent junctions and, at the same time, instant molecular arrangements in the liquid become permanent structures in the rubber. The end product is ideally composed of a ϕ volume fraction of elastically active strands (i.e., internal chain segments with both ends attached to the network) of molecular weight M_c and a $(1 - \phi)$ volume fraction of tethered chains of the same size belonging to segments with one end fixed on the network and the other free to move. The total number of chains per unit volume (ν) and the contributing population densities of strands (ν_S) and dangling ends (ν_D) are given by the following relationships:

$$\nu = \rho N_A / M_c \tag{1a}$$

$$\nu = \nu_S/\phi = \nu_D/(1 - \phi) \tag{1b}$$

where ρ is the polymer density and N_A the Avogadro number.

Increase in the cross-link density causes a decrease in M_c and a corresponding increase in ϕ. In order to investigate the way ϕ and M_c relate with other network characteristics, a detailed network architecture should be stipulated. If, for example, it is assumed that the network was formed by the tetrafunctional cross-linking of linear chains of molecular weight M and that the dangling chains are the loose ends of these primary molecules, then[2]

$$\phi = 1 - 2M_c/M \tag{2}$$

Langley[3] and Pearson and Graessley[4] have recognized that eq 2 overestimates the actual ϕ values and have modified it to account for the fact that elastically active strands should not only terminate on chemical cross-links but must also lead to the gel structure.

On the other hand, it is often suggested that elastomeric materials are composed of interacting micronetworks formed by consecutive generations of f-functional branches.[5] By assuming that extensive molecular interpenetration assures that all internal segments are elastically active, it can be shown that

$$1 - \phi = 1/(f - 1) \tag{3}$$

As long as the ability of the chains to interact with each other is not saturated with permanent junctions, entanglements coexist with cross-links and it is reasonable to assume that the network strengthening effects of cross-links and trapped entanglements are additive.[6,7] The physical parameter controlling the entanglement formation along a fixed or a tethered chain is the molecular weight between entanglements, M_e, a material constant depending on the chain flexibility of the polymeric species and its concentration.[8]

As first suggested in the de Gennes–Doi–Edwards theory for liquid polymers,[9-11] the effect of the entanglements confining a tethered chain is modeled as a cage of a mesh size proportional to M_e. This cage restricts the lateral motions of the chain but does not affect the displacements along its contour length. In the case of fixed strands, however, the part of the confining cage formed by cross-links or trapped entanglements is inescapably attached to the chain. For a more quantitative description of the intermolecular interactions, the contour length L of a strand (S) or a dangling chain (D) is divided to N_I independent steps of length a (Figures 2a and 3a):

$$L_I = N_I a \tag{4}$$

where (I = S, D) and N_S and N_D are the number steps per strand and dangling segment, respectively.

0024-9297/89/2222-0284$01.50/0

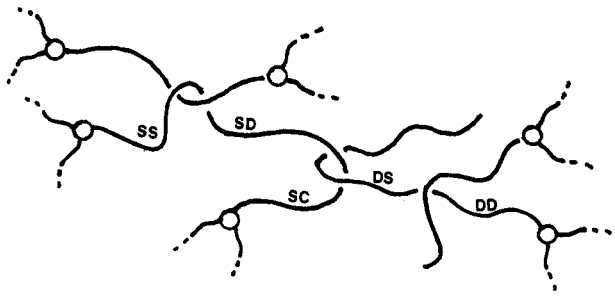

Figure 1. Entanglements in a polymer network involving internal strands and dangling chains. Circles represent cross-links, line intersections are entanglements, and dashed lines signify continuation of the network structure. Letter symbols classify the primitive steps according to their location and cause of existence (see text).

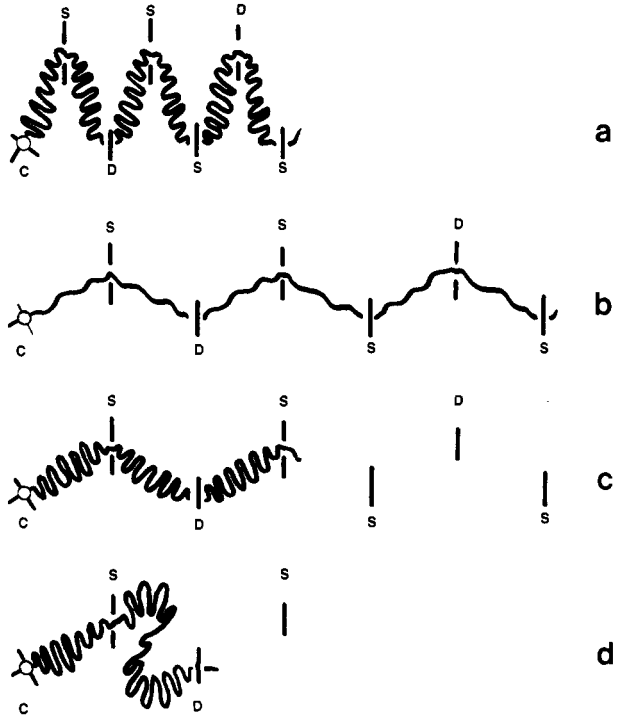

Figure 2. Tethered chain (a) at rest, (b) just after the strain imposition, (c) after equilibration through retraction, and (d) during relaxation through path fluctuations. Letter symbols signify a cross-link (C), an entanglement with a cross-linked strand (S), or an entanglement with a dangling chain (D).

Assuming that the cross-linking does not change the mesh size of the network, each segment has the following number of primitive steps at equilibrium:

$$N_S - 1 = N_D = N \tag{5a}$$

$$N = M_c/M_e \tag{5b}$$

The size of each step can be evaluated as a product of a random walk of N_e participating monomers:

$$a^2 = N_e b^2 = (M_e/m_0)b^2 \tag{6}$$

where m_0 and b are the molecular weight and the (bond) length of a monomer and N_e the number of mers between entanglements.

It is important to observe that due to the variety of chain interactions, the qualitative equivalence between steps characterizing free chains in a polymer liquid does not apply in the case of a network with chain defects. Here the primitive steps can be subdivided according to their location and cause of existence. The steps due to entanglements can be caused by an interaction either with a strand or with a tethered chain. In other words, if N_{IJ} represents the number of steps belonging to an I chain and caused by a J constraint and if C stands for a cross-link, S for a strand, and D for a dangling segment, then the following equations are valid:

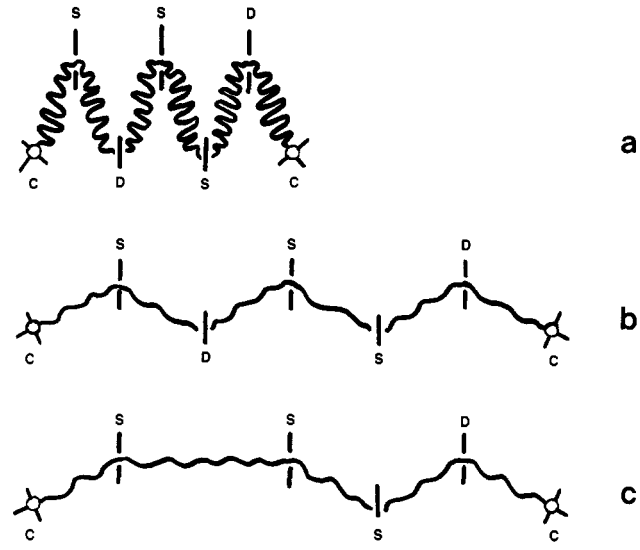

Figure 3. Cross-linked strand (a) at rest, (b) just after the strain imposition, and (c) during relaxation by constraint release due to the motion of the dangling chains. Letter symbols are the same as in Figure 2.

$$N_{SC} = 1 \tag{7a}$$

$$N_{SS} = N_{DS} = \phi N \tag{7b}$$

$$N_{DD} = N_{SD} = (1 - \phi)N \tag{7c}$$

All these different types of steps are illustrated in Figure 1.

Using the above information, the following balancing relationships can easily be verified for the fixed and tethered segments in the network:

$$N_S = N_{SC} + N_{SS} + N_{SD} = 1 + N \tag{8a}$$

$$N_D = N_{DD} + N_{DS} = N \tag{8b}$$

In equilibrium or under deformation all SC and SS steps remain indestructible since they are caused by either cross-links or entanglements trapped between them. This is not the case for the steps associated with the tethered segments (DS and DD), which are continuously dissolved and recreated, subject to the Brownian motion of the dangling ends.[9,11-13] Due to physical symmetry, SD steps are also destroyed at a rate identical with the one by which DS steps are released.[11,14-18] The disengagement of the free ends and the accompanied constraint release affect the time evolution of the stress response under a constant macroscopic deformation since, at any instant, the stress is proportional to the surviving memory of the initial confinement, at the moment of the strain imposition.

The Stress Calculation

On application of an instantaneous deformation to the material, all chain segments are stretched and oriented affinely according to the macroscopic deformation (Figures 2b and 3b). It is assumed that at this stage, all cross-links and chain entanglements are equally effective in storing energy. Each network step contributes independently to the stress (τ_{ij}), which for sufficiently small deformations, can be evaluated from the classical theory of rubber elasticity[19]

$$\tau_{ij} = (\tau_{ij})_S + (\tau_{ij})_D = 3k_B T(\nu_S N_S + \nu_D N_D)\left\langle \frac{r_i r_j}{N_e b^2} \right\rangle \tag{9}$$

where i and j signify the particular components of the stress tensor ($i, j = 1, 2, 3$) and r is the end to end distance of a step of initial size r_0, subject to Gaussian chain statistics and stretched due to a displacement that is described by the deformation gradient tensor $\mathbf{E}$:

$$\mathbf{r} = \mathbf{E}\cdot\mathbf{r}_0 = \mathbf{E}\cdot a\mathbf{u} \tag{10}$$

Upper and lower case bold face symbols signify a tensor or a vector, respectively. The symbol $\langle\ \rangle$ represents the average taken over all directions of the unit vector $\mathbf{u}$, and k_B is the Boltzmann constant. Combination of eq 9 with eq 1, 5, 6, and 10 gives the instantaneous value of the stress just after the strain imposition:

$$\tau_{ij}(t = 0^+) = 3\rho RT(\phi/M_c + 1/M_e)R_{ij} \tag{11a}$$

$$R_{ij} = \langle(\mathbf{E}\cdot\mathbf{u})_i(\mathbf{E}\cdot\mathbf{u})_j\rangle \tag{11b}$$

where t is the time and R the gas constant.

Subsequently, the two material phases react to the disturbance in their own characteristic manner. Dangling branches rearrange their conformations with the relative freedom provided by the availability of an uncross-linked end. On the other hand, fixed stands simply redistribute their total number of mers along a deformed path in order to respond to segmentational changes imposed by the relaxing branches with which they associate.

The pivotal quantity in analyzing the evolving topology of a strained network is the number of original ($t = 0$) DS steps still in existence at time t. The N_{DS} dependence on the deformation intensity and time should follow the same laws outlined for the relaxation of a single tethered chain surrounded by a permanent network. The lack of a second cross-linked end obliges a dangling segment to retract along its path, thus reducing its contour length from the elongated value of $L\langle|\mathbf{E}\cdot\mathbf{u}|\rangle$ to the equilibrium value[10] L (Figure 2c). The retracting motion of the chain takes place while the surroundings remain affinely deformed and stops when the monomer density per unit arc length is restored to its equilibrium value, N_e/a.[10,20,21] This determines the size (N'_{eDS}) and the number (N'_{DS}) of the surviving steps at the end of the equilibration stage ($t = t_e$):

$$(N'_{eDS})/(a|\mathbf{E}\cdot\mathbf{u}|) = N_e/a \tag{12}$$

$$N'_{DS} = \phi N_c/\langle N'_{eDS}\rangle = \phi N_D/\langle|\mathbf{E}\cdot\mathbf{u}|\rangle \tag{13}$$

where a prime denotes a postequilibration value and N_c is the number of mers between cross-links, or between a cross-link and a free end, $N_c = M_c/m_0$.

The time, t_e, required for a tethered chain to equilibrate is four times longer than the corresponding time for a free chain of the same size;[11] yet equilibration may be assumed an instantaneous process when compared with the time scale of the relaxation completion. This relaxation is accomplished through surplus chain fluctuations outside the cage, a process which temporarily shortens the confined path and, therefore, causes a loss of original steps and an equivalent stress decay (Figure 2d):

$$N'_{DS}(t \geq t_e) = N'_{DS}(t = t_e)F(t) = \phi N_D F(t)/\langle|\mathbf{E}\cdot\mathbf{u}|\rangle \tag{14}$$

where $F(t)$, the fraction of the original path still occupied by the chain, is a decreasing function of time ($1 \geq F(t) \geq 0$), predicted by a variety of theories referring to the dynamics of a tethered chain in a permanent network environment.[9,11-13] Experimental evidence,[22-24] supported by recent theoretical findings,[25,26] indicates that

$$F(t \geq t_m) \simeq (t_m/t)^m \tag{15}$$

where m and t_m are material parameters ($m \sim 10^{-1}$) and $t_m{}^m$ is inversely proportional to the square of the cross-link density. Simple scaling arguments suggest that for $F(t_e) = 1$, t_m should be equal to t_e. It should be made clear that eq 15 pertains to polydisperse segments, while the present work assumes monodispersity. The adoption of a realistic, simple, and well-documented expression for the time dependence of the relaxation progression was, however, necessary in order to assess the long-lasting implications of the presence of dangling ends on the mechanical properties of the network (see Discussion).

The knowledge of the mechanism of the DS step reduction may be used to calculate the number of steps of any kind, N'_{IJ}, at any time after the strain imposition. This is accomplished by stipulating randomly associating S and D segments and, therefore, by assuming that the ratio of J steps over I steps along a single I chain is equal to the corresponding ratio in the total step population of the network. Thus, for (I,J) = (S,D)

$$\frac{N'_{IJ}}{N'_{II}} = \frac{\nu_J(N'_{JI} + N'_{JJ})}{\nu_I(N'_{II} + N'_{IJ})} \tag{16}$$

This expression, which is evidently satisfied by the conditions at rest (eq 7b,c), may be recast in a more convenient form:

$$\nu_S N'_{SD} = (\nu_S N'_{SS}\nu_D N'_{DD})^{1/2} = \nu_D N'_{DS} \tag{17}$$

Strands anchored with both ends on the network are not able to move; therefore the SS and SC step populations remain intact ($N'_{SS} = N_{SS}$ and $N'_{SC} = N_{SC}$). Then, from eq 14 and 17, the following results are obtained:

$$N'_{SC} = 1 \tag{18a}$$

$$N'_{SS} = \frac{N'_{DS}}{F(t)}\langle|\mathbf{E}\cdot\mathbf{u}|\rangle = \phi\frac{M_c}{M_e} \tag{18b}$$

$$\frac{N'_{DD}}{F^2(t)}\langle|\mathbf{E}\cdot\mathbf{u}|\rangle^2 = \frac{N'_{SD}}{F(t)}\langle|\mathbf{E}\cdot\mathbf{u}|\rangle = (1 - \phi)\frac{M_c}{M_e} \tag{18c}$$

It is observed that the DD steps are renewed faster than the DS steps due to the inevitable release of some of their confining constraints and that the disengagement of DS steps causes a destruction of SD steps at an equal rate (Figure 3c). Equation 18 implies that a primitive step becomes elastically ineffective at the same instant the entanglement, which causes it, is released. This approximation, first introduced by Marrucci[15] and Viovy,[17] assumes that constraint release and chain disengagement have an identical spectrum of relaxation times, instead of the more realistic Rouse-type relaxation spectrum suggested by Graessley[11] and by Rubinstein, Helfand, and Pearson.[18]

In order to calculate the stress contribution due to the surviving steps, the value for the postequilibration step length, $\mathbf{r}'$, should also be known. Since monomer units are neither created nor destroyed during the relaxation process, reduction of the number of the IJ steps is accompanied by an equivalent increase of the average step size:

$$\langle N'_{eIJ}\rangle = N_e\frac{N_{IJ}}{N'_{IJ}} \tag{19}$$

In an idealized description of the network weakening effect of constraint release, eq 19 implies that this phenomenon affects exclusively the size of the steps associated with dangling ends, while it leaves the size of the SS and SC steps intact. The size of each individual step also varies according to its relative orientation with respect to the direction of the macroscopic deformation:[11]

$$N'_{eIJ} = \langle N'_{eIJ}\rangle\frac{|\mathbf{E}\cdot\mathbf{u}|}{\langle|\mathbf{E}\cdot\mathbf{u}|\rangle} \tag{20}$$

The part of the stress due to the IJ segments, $(\tau_{ij})_{IJ}$, is then equivalent to the stress generated by the imposition of a displacement gradient $\mathbf{E}$ to a network composed of $\nu_I N'_{IJ}$ strands per volume and with an average strand size (at rest) equal to $|\mathbf{r}'_0| = a' = \langle N'_{eIJ}\rangle^{1/2} b$:

$$(\tau_{ij})_{IJ}(t \geq t_e) = 3k_B T \nu_I N'_{IJ} \left\langle \frac{r'_i r'_j}{N'_{eIJ} b^2} \right\rangle = 3k_B T \nu_I N'_{IJ} H_{ij}(\mathbf{E}) \alpha(\mathbf{E}) \quad (21)$$

where

$$\alpha(\mathbf{E}) = \langle |\mathbf{E}\cdot\mathbf{u}| \rangle \quad (22a)$$

and

$$H_{ij}(\mathbf{E}) = \left\langle \frac{(\mathbf{E}\cdot\mathbf{u})_i (\mathbf{E}\cdot\mathbf{u})_j}{|\mathbf{E}\cdot\mathbf{u}|} \right\rangle \quad (22b)$$

It is assumed that each step population contributes independently to the total stress formation:

$$\tau_{ij}(t) = \sum_I \sum_J (\tau_{ij}(t))_{IJ} \quad (23)$$

By combination of eq 21 and 23 with eq 1, 5, 8, and 18, the following expression is derived for the total stress as a function of strain, time, and network architecture:

$$\tau_{ij}(t) = 3RT\rho \left\{ \frac{\phi}{M_c} + \frac{1}{M_e} \left[\phi + (1-\phi) \frac{F(t)}{\alpha(\mathbf{E})} \right]^2 \right\} H_{ij}(\mathbf{E}) \alpha(\mathbf{E}) \quad (24)$$

The time-invariant terms represent the elastic effects of cross-links and trapped entanglements while the time-dependent term is due to the perishable steps which are either lying on or formed by tethered chains. Equation 24 may also be expressed in terms of the classical result for the elasticity modulus of a rubber with an identical cross-link density ($G_c = RT\rho\phi/M_c$) and the rubbery plateau modulus ($G_N^0 = RT\rho/M_e$) assumed by the same polymeric species in the fluid state:

$$\tau_{ij}(t) = 3 \left\{ G_c + G_N^0 \left[\phi + (1-\phi) \frac{F(t)}{\alpha(\mathbf{E})} \right]^2 \right\} H_{ij}(\mathbf{E}) \alpha(\mathbf{E}) \quad (25)$$

The implications of these results are examined in the next section.

Discussion

The consistency of the present theory with earlier theoretical findings is demonstrated by examining its validity at extreme cases of material behavior. By assuming that the disengagement of all tethered segments reaches completion ($F(\infty) = 0$), eq 25 reduces to the predictions by Mancke et al.[27] for the equilibrium modulus of a network with trapped entanglements (ϕ from eq 2). By letting $\phi \to 1$, the Marrucci–Graessley expression for the elasticity of rubbers containing entanglements is retrieved.[11,21] Finally, as the presence of cross-links is suppressed ($\phi \to 0$) a modification of the de Gennes–Doi–Edwards theory predictions for the viscoelasticity of star-shaped and linear polymer liquids is obtained:

$$\tau_{ij}(t) = 3 \frac{RT\rho}{M_e} \frac{H_{ij}(\mathbf{E})}{\alpha(\mathbf{E})} F^2(t) \quad (26)$$

For the case of linear chains, where reptation is the dominant mechanism of the chain disengagement, $F(t)$ should be replaced by $R(t)$, the time decaying fraction of the original steps not yet eliminated by reptation. Equation 26 differs from the original theory[9-11] by suggesting that the rate of the macromolecular relaxation of a free polymer in an environment of similar molecules is equal to the square of the relaxation rate of the same polymer in an environment of invariable topology (i.e., in a permanent network). This result has first been derived by Marrucci[15] and Viovy.[17]

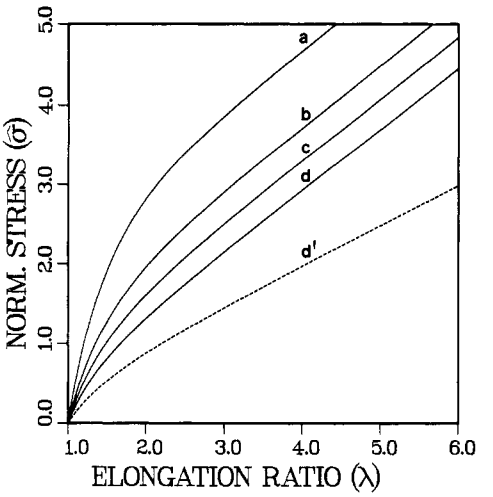

Figure 4. Normalized nominal stress, $\hat{\sigma} = (\tau_{11} - \tau_{22})/(\lambda RT\rho/M_c)$, under uniaxial elongation, calculated from eq 27 for $\phi = M_e/M_c = 0.5$ and $F(t)$ (or F_0) equal to (a) 1.0, (b) 0.50, (c) 0.25, and (d) 0.0. For $F(t)$ given by eq 15 with $m = 0.07$ and $t_m = 0.02$ s, these correspond to $t = 0.02$ s, 7 min, 3 months, and ∞. The dashed curve (d') shows the classical theory predictions at equilibrium (eq 28 and 31).

True tensile stresses (i.e., force/deformed cross-sectional area) after sudden uniaxial elongations for a range of extension ratios ($6 > \lambda > 1$) are calculated from eq 24:

$$\tau_{11} - \tau_{22} = 3RT\rho[K_1 \alpha(\mathbf{E}) + K_2(\mathbf{E},t)](H_{11} - H_{22}) \quad (27a)$$

where

$$K_1 = \phi/M_c + \phi^2/M_e \quad (27b)$$

and

$$K_2(\mathbf{E},t) = (1-\phi)[2\phi + (1-\phi)F(t)/\alpha(\mathbf{E})]F(t)/M_e \quad (27c)$$

They are plotted in Figure 4 in terms of the nominal tensile stress (force/undeformed cross-sectional area), $\sigma = (\tau_{11} - \tau_{22})/\lambda$, which is the standard way of presenting the experimental results. The calculated values refer to a rubber with $\phi = M_e/M_c = 1/2$. The corresponding predictions of the classical theory at equilibrium[2] are also plotted for comparison:

$$\sigma = (\tau_{11} - \tau_{22})/\lambda = 3RT\rho(\phi/M_c)(R_{11} - R_{22})/\lambda \quad (28)$$

It is reminded that for this type of deformation geometry[21]

$$\alpha(\mathbf{E}) = \frac{\lambda}{2} \left(1 + \frac{\ln(\lambda^{3/2} + (\lambda^3 - 1)^{1/2})}{\lambda^{3/2}(\lambda^3 - 1)^{1/2}} \right) \quad (29)$$

$$H_{11} - H_{22} = \frac{\lambda(2\lambda^3 + 1)}{4(\lambda^3 - 1)} \left(1 - \frac{4\lambda^3 - 1}{2\lambda^3 + 1} \frac{\ln(\lambda^{3/2} + (\lambda^3 - 1)^{1/2})}{\lambda^{3/2}(\lambda^3 - 1)^{1/2}} \right) \quad (30)$$

and

$$R_{11} - R_{22} = (\lambda^2 - \lambda^{-1})/3 \quad (31)$$

In agreement with experimental observations from earlier[2] and more recent studies[28-30] the calculated stress values are systematically higher than the ones obtained from the classical theory. This is attributed to the rein-

forcing effect of the trapped entanglements. Valles and Macosko[29] report that in a series of almost perfect poly(dimethylsiloxane) networks the topological reinforcement to the equilibrium modulus is equal to $0.75G_N^0$, a value close to the $0.80G_N^0$ calculated from eq 27 for $\phi = 1$ and $\lambda \to 1$.

In addition to predicting an increase in the material rigidity due to the presence of physical junctions, the present theory attempts to explain the observed deviations from the neo-Hookean behavior, manifested by an increased curvature at the origin of the experimental stress–strain curve.[31] By recalling that for a uniaxial elongation $\alpha(\mathbf{E})$ is an increasing function of strain ($\alpha \to \lambda/2$ for large enough deformations) and that the product $\alpha(\mathbf{E})(H_{11} - H_{22})$ can be approximated by $4(\lambda^2 - \lambda^{-1})/15$, it is observed that eq 27 produces an expression similar (though not identical) in form and strain dependence to the well-established Mooney–Rivlin (MR) phenomenological model:[31]

$$(\tau_{11} - \tau_{22})_{MR} = 2(C_1 + C_2/\lambda)(\lambda^2 - \lambda^{-1}) \qquad (32)$$

The K_2 term in eq 27, like C_2, represents the deviations from the neo-Hookean behavior (eq 28 and 31). In this respect, the theoretical predictions are consistent with the experimental evidence, which reveals that these deviations decrease with the elapsed time after the strain imposition[32-34] and disappear in rubbers with end-linked segments ($\phi \simeq 1$).[32]

Following this logic, and since $F(\infty) = 0$, it is to be expected that the strain dependence of the stress at equilibrium is described by the neo-Hookean law ($C_2 = 0$). This is apparently contradicted by the results of numerous experimental investigations which indicate that $C_2 \neq 0$. Nevertheless, comparison of the conventional time scales used in these studies with the sluggish rate of the molecular relaxation suggests that it is questionable whether real steady-state conditions have been achieved at the end of these measurements. In order to appreciate the enormous time requirements for the complete conformational renewal of a tethered chain in a relatively strong network, let us assume that eq 15 is valid for the entire relaxation range. For $m = 0.073$ and $t_m = 0.016$ s (i.e., sample A-20 of ref 23), $F(t)$ reaches the 41% of its initial value within an hour after the strain imposition. Yet, for an $F(t)$ reduction to 32%, 25%, and 21% the respective waiting periods equal a day, a month, and a year.

It is, therefore, plausible that that the C_2 values extracted from experiments under "equilibrium" conditions are actually manifestations of the incomplete relaxation of the free ends. If F_0 signifies the $F(t)$ value at the end of such an experiment and $K_{20} \equiv K_2(\mathbf{E} \to 1)$, then

$$2C_2 \simeq 0.8RT\rho K_{20} = 0.8(1 - \phi)[2\phi + (1 - \phi)F_0]F_0G_N^0 \qquad (33)$$

An estimate for the extent of the relaxation completion may be obtained from the experimental results of Pearson and Graessley[30] on well-characterized ethylene–propylene copolymer networks ($\lambda < 1.3$). For these materials the topological contribution to the neo-Hookean term is equal to 0.31 MPa, a value independent of the molecular weight of the primary chains. For the same polymer in the fluid state, $G_N^0 = 1.72$ MPa and, therefore, (from eq 25) $\phi = (0.31/0.8G_N^0)^{1/2} = 0.475$. The average value for the term representing the deviations from neo-Hookean behavior is 0.29 MPa and thus, from eq 33, $F_0 = 0.35$. For $t_m \sim 0.01$ s and for reported relaxation times of 2 days, it is estimated (from eq 15) that $m \simeq 0.06$. The invariance of the elongation ratio under constant external force for an additional month was used as a criterion for the establishment of equilibrium conditions. According to eq 25 (for $G_c \simeq 0.3$ MPa), however, the increase of λ during that extra period would have been less than 1%, a change too small to be detected.

The ratio K_{20}/K_1 is a measure of the relative contribution of the time-dependent term to the final stress value:

$$\frac{K_{20}}{K_1} = \frac{(1 - \phi)[2\phi + (1 - \phi)F_0]F_0}{\phi(M_e/M_c + \phi)} \qquad (34)$$

It has already been mentioned that increase in the cross-link density causes a decrease in M_c and a corresponding increase in ϕ. By assuming that the molecular weight between cross-links scales as $M_c \sim \beta/\phi$ (β is a proportionality constant), the following relationship is obtained:

$$\frac{C_2}{C_1} \simeq \frac{K_{20}}{K_1} \sim \frac{M_c - \beta}{M_e + \beta}\left[2 + \left(\frac{M_c}{\beta} - 1\right)F_0\right]F_0 \qquad (35)$$

This result conforms with experimental observations indicating that the relative importance of the deviations from the neo-Hookean behavior increases by reducing (a) the degree of cross-linking ($1/M_c$ or ϕ),[35] (b) the presence of a diluent during the network formation (M_e),[35] and (c) the molecular rigidity of the primary chains (M_e).[36]

It should, finally, be reminded that a basic assumption in this work is that all structural units of the network are of the same size (M_c). Although experience indicates that the effect of polydispersity is less profound on the strain-dependent properties than on the time dependence of the viscoelastic response,[25,26] an improved theory should also include the presence of internal strands and dangling chains covering a wide distribution of molecular weights. By inspecting eq 24, it is clear that polydispersity should primarily affect the term due to cross-links and the time-dependent part of the entanglement term. An approximate result toward this direction may thus be obtained by replacing M_c with its number-average value and by adopting an expression for $F(t)$ able to accommodate polydispersity (e.g., eq 15).

Conclusions

The effects of the presence of trapped entanglements and chain defects on the stress response of a deformed polymeric network, at different relaxation stages, has been theoretically investigated. A consistent way of coupling the strain and time dependence in a constitutive relationship has been developed. The stress value is determined by the number densities of trapped entanglements, internal stretched segments, and oriented dangling chains. This last contribution provides a molecular explanation to the observed deviations from the neo-Hookean behavior. It is predicted that the relative importance of these deviations decreases by increasing the cross-link density, the interentanglement distance, and the elapsed time after the strain imposition. These predictions are in agreement with experimental observations.

References and Notes

(1) Ferry, J. D. *Viscoelastic Properties of Polymers*, 3rd ed.; Wiley: New York, 1980; Chapters 10, 13, 14.
(2) Flory, P. J. *Principles of Polymer Chemistry*; Cornell University: Ithaca, NY; 1953; Chapter 11.
(3) Langley, N. R. *Macromolecules* **1968**, *1*, 348.
(4) Pearson, D. S.; Graessley, W. W. *Macromolecules* **1978**, *11*, 528.
(5) Graessley, W. W. *Macromolecules* **1975**, *8*, 186, 865.
(6) Bueche, A. M. *J. Polym. Sci.* **1956**, *19*, 297.
(7) Mullins, L. *J. Appl. Polym. Sci.* **1959**, *2*, 1.
(8) Graessley, W. W. *Adv. Polym. Sci.* **1974**, *16*, 1.
(9) de Gennes, P.-G. *Scaling Concepts in Polymer Physics*; Cornell University: Ithaca, NY; 1979; Chapter 8.

(10) Doi, M.; Edwards, S. F. *J. Chem. Soc., Faraday Trans.* **1978**, *74*, 1802.
(11) Graessley, W. W. *Adv. Polym. Sci.* **1982**, *47*, 67.
(12) Doi, M.; Kuzuu, N. Y. *J. Polym. Sci., Polym. Lett. Ed.* **1980**, *18*, 775.
(13) Pearson, D. S.; Helfand, E. *Macromolecules* **1984**, *17*, 888.
(14) Viovy, J. L.; Monnerie, L.; Tassin, J. F. *J. Polym. Sci., Polym. Phys. Ed.* **1983**, *21*, 2427.
(15) Marrucci, G. *J. Polym. Sci., Polym. Phys. Ed.* **1985**, *23*, 159.
(16) Viovy, J. L. *J. Polym. Sci., Polym. Phys. Ed.* **1985**, *23*, 2423.
(17) Viovy, J. L. *J. Phys. (Les Ulis, Fr.)* **1985**, *46*, 847.
(18) Rubinstein, M.; Helfand, E.; Pearson, D. S. *Macromolecules* **1987**, *20*, 822.
(19) Bird, R. B.; Armstrong, R. C.; Hassager, O.; Curtiss, C. F. *Dynamics of Polymeric Liquids*; Wiley: New York, 1977; Vol. 2.
(20) Ziabicki, A. *Colloid Polym. Sci.* **1976**, *254*(1), 1.
(21) Marrucci, G. *Rheol. Acta* **1979**, *18*, 193.
(22) Chasset, R.; Thirion, P. *Proceedings of the Conference on Physics of Non-Crystalline Solids*; Prins, J. A., Ed.; North-Holland: Amsterdam, 1965; p 35.
(23) Dickie, R. A.; Ferry, J. D. *J. Phys. Chem.* **1966**, *70*, 2954.
(24) Plazek, D. J. *J. Polym. Sci., Polym. Phys. Ed.* **1966**, *4*, 745.
(25) Curro, J. G.; Pincus, P. *Macromolecules* **1983**, *16*, 559.
(26) Curro, J. G.; Pearson, D. S.; Helfand, E. *Macromolecules* **1985**, *18*, 1157.
(27) Mancke, R. G.; Dickie, R. A.; Ferry, J. D. *J. Polym. Sci., Polym. Phys. Ed.* **1968**, *6*, 1783.
(28) Dossin, L. M.; Graessley, W. W. *Macromolecules* **1979**, *12*, 123.
(29) Valles, E. M.; Macosko, C. W. *Macromolecules* **1979**, *12*, 673.
(30) Pearson, D. S.; Graessley, W. W. *Macromolecules* **1980**, *13*, 1001.
(31) Treloar, L. R. G. *The Physics of Rubber Elasticity*, 3rd ed.; Clarendon: Oxford, 1975.
(32) Kraus, G.; Moczygemba, G. A. *J. Polym. Sci., Part A* **1964**, *2*, 277.
(33) Ciferri, A.; Flory, P. J. *J. Appl. Phys.* **1959**, *30*, 1498.
(34) Smith, T. L. *J. Polym. Sci., Part C* **1967**, *16*, 841.
(35) Mark, J. E. *Rubber Chem. Technol.* **1975**, *48*, 495.
(36) Boyer, R. F.; Miller, R. L. *Polymer* **1987**, *28*, 399.

Diffusion of Various Dialkyl Phthalate Plasticizers in PVC

Robson F. Storey,* Kenneth A. Mauritz, and B. Dwain Cox

Department of Polymer Science, University of Southern Mississippi, Southern Station Box 10076, Hattiesburg, Mississippi 39406-0076. *Received April 27, 1988; Revised Manuscript Received July 19, 1988*

ABSTRACT: Diffusion coefficients of several *n*-alkyl phthalates and several commercial phthalate plasticizers in PVC were measured over the temperature range $60 \leq T \leq 100$ (°C) by using a mass uptake technique. The values were observed to be in the range 2×10^{-10} to 8×10^{-7} cm^2/s. With other conditions held constant, diffusion coefficients were found to increase with temperature, decrease with increase in alkyl group length, and decrease with increase in alkyl group branchiness. Diffusion temperature dependence was observed to follow an Arrhenius relationship over the temperature range studied, but with a change in slope at the glass transition of PVC. The activation energy for diffusion of di-*n*-hexyl phthalate was found to be 22 kcal/mol above the PVC glass transition and 7.9 kcal/mol below it. Among the *n*-alkyl phthalate series, ln (diffusion coefficient) was found to be approximately linear with respect to the number of carbons in the *n*-alkyl chain.

Introduction

The diffusion of large penetrant molecules within polymers is an important process which directly impacts such technologies as the processing of various additives into polymers, membrane liquid/liquid separations, the transport of biologically active molecules through polymer matrices in controlled-release applications, and many others. We are currently developing a penetrant shape-dependent, largely free volume based diffusion model that utilizes theoretical conformational analysis[1,2] to predict diffusion coefficients (D) for large penetrant molecules within amorphous, cross-linked, or semicrystalline polymers above their glass transition temperatures (T_g).

An important application for this model, and one which concerns us presently, is the diffusion of plasticizer molecules into and out of poly(vinyl chloride) (PVC). PVC is one of the most important commodity industrial polymers, and in most applications its properties are modified by compounding with a compatible plasticizer. Introduction of the plasticizer into PVC usually takes place in a dry blending operation in which suspension-polymerized PVC particles are heated and rapidly sheared with plasticizer and other compounding ingredients in a mixer. It has been suggested that the rate of dry blending is in fact diffusion controlled;[3,4] thus the rate of diffusion of a particular plasticizer into PVC determines the required dry blending time, which directly affects processing costs.

Plasticizer diffusion also affects the longevity of plasticized PVC goods. Just as plasticizer diffusion into PVC affects the ease of processing, plasticizer diffusion out of the processed vinyl compound determines to a great extent the useful lifetime of the article.

There exists a great volume of literature dealing with the thermodynamics and kinetics of the uptake of various commercial plasticizers in PVC resin particles as well as in solvent-cast and hot-pressed PVC films. While it is quite impossible to enumerate all of the studies performed in this vast general area, we will summarize only those we feel most closely relate to the work reported herein.

In an early study, Knappe determined diffusion coefficients of DOP in PVC films by measuring index of refraction as a function of time.[5] At 80 °C, for example, D steadily increased from 6.1×10^{-11} to 6.7×10^{-8} cm^2/s as the plasticizer concentration increased from 10 to 80 wt %. At 100 °C, D increased from 5.6×10^{-10} to 1.4×10^{-7} cm^2/s over the same concentration range. Furthermore, ln D vs T^{-1} curves were quite linear, and the energies of activation for diffusion decreased from 30.1 to 8.7 kcal/mol from 10 to 80 wt % DOP.

Using a procedure similar to that reported in this work, Grotz determined D values from the slopes of plasticizer uptake vs (time)$^{1/2}$ lines obtained by using disks of suspension-polymerized PVC immersed in excess DOP in the temperature range 65–85 °C.[6] D increased, in Arrhenius fashion, from 9.6×10^{-11} to 3.0×10^{-8} cm^2/s from 65 to 85 °C, respectively, after an initial induction period, with an activation energy of 60 kcal/mol. In contrast with Knappe's results, Grotz's activation energy was somewhat high and appeared to be independent of incorporated plasticizer concentration.

It is necessary for us, at this time, to point out that the equation used by Grotz is in fact based on a solution to the diffusion equation derived from boundary conditions that are inappropriate for the situation of a disk immersed

0024-9297/89/2222-0289$01.50/0